

Is integrated ^{18}F -FDG PET/MRI superior to ^{18}F -FDG PET/CT in the differentiation of incidental tracer uptake in the head and neck area?

Benedikt Michael Schaarschmidt
Benedikt Gomez
Christian Buchbender
Johannes Grueneisen
Felix Nensa
Lino Morris Sawicki
Verena Ruhlmann
Axel Wetter
Gerald Antoch
Philipp Heusch

PURPOSE

We aimed to investigate the accuracy of ^{18}F -fluorodeoxyglucose positron emission tomography/magnetic resonance imaging (^{18}F -FDG PET/MRI) compared with contrast-enhanced ^{18}F -FDG PET/computed tomography (PET/CT) for the characterization of incidental tracer uptake in examinations of the head and neck.

METHODS

A retrospective analysis of 81 oncologic patients who underwent contrast-enhanced ^{18}F -FDG PET/CT and subsequent PET/MRI was performed by two readers for incidental tracer uptake. In a consensus reading, discrepancies were resolved. Each finding was either characterized as most likely benign, most likely malignant, or indeterminate. Using all available clinical information including results from histopathologic sampling and follow-up examinations, an expert reader classified each finding as benign or malignant. McNemar's test was used to compare the performance of both imaging modalities in characterizing incidental tracer uptake.

RESULTS

Forty-six lesions were detected by both modalities. On PET/CT, 27 lesions were classified as most likely benign, one as most likely malignant, and 18 as indeterminate; on PET/MRI, 31 lesions were classified as most likely benign, one lesion as most likely malignant, and 14 as indeterminate. Forty-three lesions were benign and one lesion was malignant according to the reference standard. In two lesions, a definite diagnosis was not possible. McNemar's test detected no differences concerning the correct classification of incidental tracer uptake between PET/CT and PET/MRI ($P = 0.125$).

CONCLUSION

In examinations of the head and neck area, incidental tracer uptake cannot be classified more accurately by PET/MRI than by PET/CT.

In many oncologic diseases, ^{18}F -fluorodeoxyglucose positron emission tomography/computed tomography (^{18}F -FDG PET/CT) has increased diagnostic accuracy in comparison to CT or magnetic resonance imaging (MRI) (1, 2). Patients benefit from the accurate detection of nodal tumor spread due to the highly accurate localization of ^{18}F -FDG tracer uptake on the corresponding and coregistered CT scan (3). Furthermore, the morphologic dataset can be of considerable value in the clarification of tracer uptake in atypical locations that cannot be classified as functional or nonmalignant on PET images alone (4). Although recommended by the latest guidelines for lymph nodes and recurrence diagnostics in head and neck cancers (5, 6), the interpretation of these scans can be difficult. Although tracer uptake in the tonsils, pharynx, and thyroid gland can be frequently found (7), the possibility of a second, unrelated malignancy, although rare, requires further investigations (8–11). Due to the complex head and neck anatomy, the low soft tissue contrast inherent to CT may be inferior to MRI in head and neck imaging (12–14). For this reason, integrated PET/MRI scanners may be advantageous (15, 16).

Apart from the possibility of combining local tumor as well as nodal and distant metastasis staging in a "one stop shop" examination, the superior soft tissue contrast of MRI could also improve the classification of incidental tracer uptake compared with PET/CT. Therefore, the aim of this study was to examine whether ^{18}F -FDG PET/MRI provides a better diagnostic accuracy in the characterization of incidental tracer uptake than ^{18}F -FDG PET/CT.

From the Department of Diagnostic and Interventional Radiology (B.M.S. ✉ benedikt.schaarschmidt@med.uni-duesseldorf.de, C.B., L.M.S., G.A., P.H.), Dusseldorf University School of Medicine, Dusseldorf, Germany; the Departments of Diagnostic and Interventional Radiology and Neuroradiology (B.M.S., J.G., F.N., A.W.) and Nuclear Medicine (B.G., V.R.), Duisburg-Essen University School of Medicine, Essen, Germany.

Received 29 December 2014; revision requested 25 March 2016; last revision received 30 April 2016; accepted 5 July 2016.

Published online 16 January 2017.
DOI 10.5152/dir.2016.15610

Table 1. MRI sequences used in the dedicated head and neck protocol in integrated PET/MRI

Pulse sequence name	Orientation	TR/TE (ms)	Slice thickness (mm)	Matrix size	FOV (mm ²)
Unenhanced T1-weighted TSE	Coronal	557/10	5	512×307	300×300
Unenhanced T1-weighted TSE	Transverse	554/11	3	512×256	260×260
T2-weighted TSE	Transverse	5340/111	3	512×256	260×260
Contrast-enhanced volume interpolated breath-hold (Dixon)	Transverse	8.57/3.69/4.92	2	480×384	270×270
Contrast-enhanced T1-weighted TSE (Dixon)	Transverse	472/16	3	480×384	260×260
Contrast-enhanced T1-weighted TSE	Coronal	669/10	5	512×307	300×300

PET/MRI, positron emission tomography/magnetic resonance imaging; TR/TE, repetition time/echo time; FOV, field of view; TSE, turbo spin-echo.

Methods

Patients

In our database, 81 patients (40 female and 41 male patients; mean age, 54.4±15 years) who underwent contrast-enhanced whole-body PET/CT examination including a dedicated head and neck protocol followed by a dedicated PET/MRI examination of the head and neck area were identified and further investigated in this retrospective analysis. The indications for PET/CT and PET/MRI comprised the following: initial tumor diagnostics (n=24), treatment monitoring (n=10), and recurrence diagnostics and follow-up (n=47). All 81 patients suffered from or had undergone treatment for tumors of the salivary glands (n=25), carcinomas of the oral and nasal cavity (n=21), thyroid cancer (n=18), carcinoma with unknown primary tumor (CUP) syndrome (n=15) and other tumor entities (n=2). The examinations were performed as part of a comparative study between PET/MRI and PET/CT, which was approved by the local ethics committee including retrospective data analysis. All patients gave their written informed consent before PET/MRI.

PET/CT

A weight-dependent ¹⁸F-FDG dose (mean activity, 260±50 MBq) was injected 60 min

prior to a contrast-enhanced, dedicated head and neck PET/CT scan which was followed by a whole-body PET/CT examination. The examinations were performed on a Biograph mCT™ (Siemens Healthcare GmbH). At the time of ¹⁸F-FDG injection, blood glucose levels were below 150 mg/dL.

For the head and neck area, CT images (slice thickness, 3 mm; pitch, 0.8) were acquired from the base of the skull to the aortic arc 40 s after the injection of 60 mL of an iodine-based contrast agent (Ultravist®, Bayer Healthcare). For head and neck imaging, the arms of the patients were positioned next to the body. For the subsequent whole-body scan, patients were encouraged to lift their arms over their head to minimize artifacts. The scan was performed from the upper thorax to the upper thighs 70 s after the additional injection of 70 mL of an iodine-based contrast agent (slice thickness: 5 mm; pitch: 1). CareDose 4DTM (presets: 210 mAs) and CareKV™ (presets: 120 kV, Siemens Healthcare GmbH) were used in both protocols to minimize radiation exposure. PET data acquisition was performed in the head and neck area for 4 min per bed position and in the rest of the body for 2 min. Images were reconstructed using the ordered subset expectation maximization (OSEM; 3 iterations and 21 subsets; Gaussian filter, 4 mm).

PET/MRI

After the PET/CT scan, a dedicated head and neck examination was performed on a Magnetom Biograph mMR™ (Siemens Healthcare GmbH), 150±47 min after ¹⁸F-FDG injection. For attenuation correction, a T1-weighted three-dimensional volume interpolated breath-hold examination (VIBE) sequence in Dixon technique was acquired in coronal orientation (TE1, 1.23 ms; TE2, 2.46 ms; TR, 3.6 ms; slice thickness, 3.12 mm; flip angle, 10°; matrix size, 192×121;

field-of-view, 500×328 mm²). The diagnostic MRI sequences comprised coronal unenhanced T1-weighted turbo spin-echo (TSE), transverse unenhanced T1-weighted TSE, transverse T2-weighted TSE, transverse contrast-enhanced VIBE and fat suppressed T1-weighted TSE sequence, and transverse contrast-enhanced T1-weighted TSE sequence (see Table 1 for further details). For contrast-enhanced images, a weight-adapted dose (0.2 mL/kg bodyweight) of gadolinium-based contrast agent (Dotarem®; Guerbet) was injected. To reduce acquisition times, generalized autocalibrating partially parallel acquisition, acceleration factor (GRAPPA) 2 was used. PET data acquisition was performed for 20 min in list mode. Just as in PET/CT, PET images were reconstructed using OSEM (3 iterations and 21 subsets; Gaussian filter, 4 mm; matrix size, 344×344).

Image analysis and reference standard

In random order, PET/CT and PET/MRI examinations were investigated for incidental tracer uptake under knowledge of the clinical indication to exclude the primary tumor and potential metastases by two readers in separate sessions using OsiriX (Pixmeo SARL). The first reader was a nuclear medicine physician with six years of PET/CT experience, the second reader was a radiologist with five years of PET/CT experience. Both readers had at least two years of experience in integrated PET/MRI reading. As symmetrical tracer uptake can be frequently observed in the Waldeyer's ring and the pharyngeal and laryngeal musculature, only asymmetrical, focal tracer uptake compared with the background found in these locations was included in the analysis.

In a second step, the PET images and the morphologic CT or MRI images were analyzed fused and side-by-side for morphologic correlates of the focal tracer uptake and the most probable diagnosis was not-

Main points

- Integrated ¹⁸F-FDG PET/MRI is considered as superior to PET/CT in head and neck imaging due to the superior soft tissue contrast.
- However, incidental ¹⁸F-FDG uptake is a common problem in hybrid imaging of the head and neck.
- According to this retrospective analysis, ¹⁸F-FDG PET/MRI is not superior to PET/CT in the characterization of incidental ¹⁸F-FDG uptake.

Table 2. Incidental tracer uptake correctly identified by PET/CT and PET/MRI in 46 lesions

Diagnosis	Correct diagnosis by PET/CT	Correct diagnosis by PET/MRI
Brown fatty tissue	17 (36.9)	17 (36.9)
Postoperative changes	4 (8.7)	5 (10.9)
Residual thymus tissue	2 (4.3)	2 (4.3)
Arthritic changes of the cervical spine	0 (0)	2 (4.3)
Reactive uptake in a nonmalignant lymph node	1 (2.2)	1 (2.2)
Mucosal uptake due to sinusitis	1 (2.2)	1(2.2)
Nonspecific muscular uptake	1 (2.2)	1 (2.2)
Malignant tumor of the thyroid gland	1 (2.2)	1 (2.2)
Arteriosclerotic plaque	1 (2.2)	1 (2.2)
Infected atheroma	0 (0)	1 (2.2)
Total	28	32

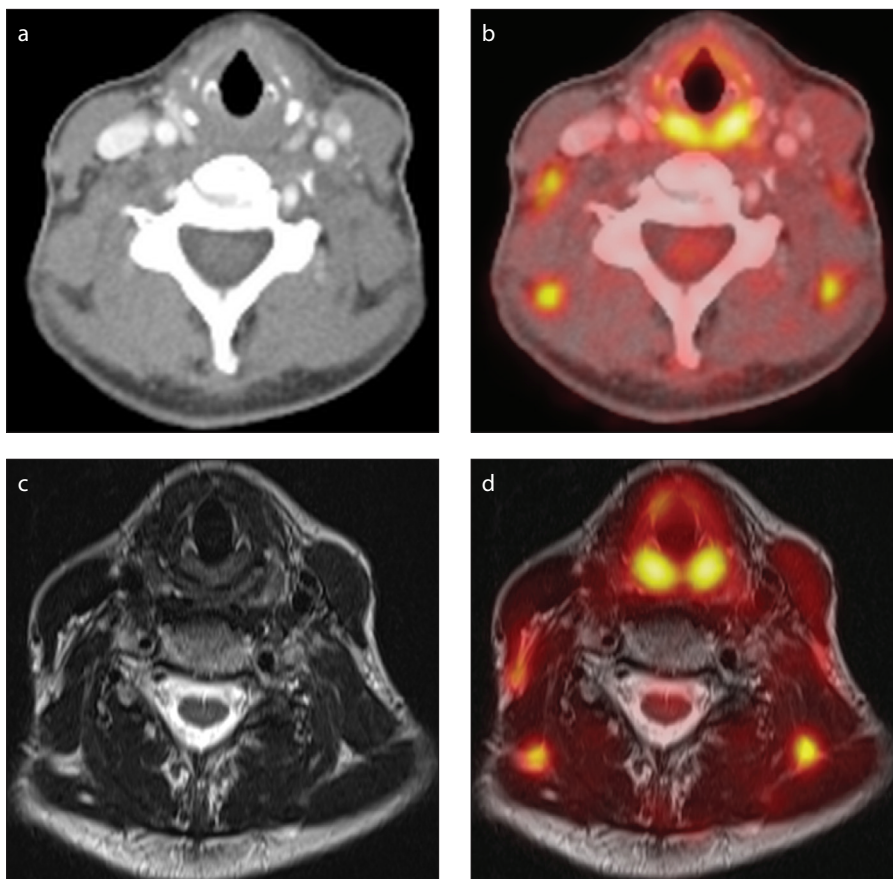


Figure 1. a–d. A 36-year-old female patient who underwent hybrid imaging for follow-up after successful treatment of tonsil cancer. Morphologic and fused images are displayed for PET/CT (**a, b**) and PET/MRI (**c, d**). While no lesions can be detected by morphologic imaging (**a, c**), all ^{18}F -FDG avid lesions are localized in the intermuscular fat in both modalities (**b, d**) and can therefore be clearly identified as brown fatty tissue in both modalities.

ed. Each finding was classified in one of the following categories: most likely benign, indeterminate, or most likely malignant (17). A finding that did not demand further follow-up due to its benign appearance or its characteristic anatomical location

in the analyzed images was considered as “most likely benign”, while a finding that was considered as malignant and needed immediate verification by endoscopy, histopathologic sampling or further imaging was considered as “most likely malignant.”

If a finding was considered as neither malignant nor typically benign in the PET/CT or PET/MRI images, it was considered as “indeterminate.” Discrepancies between both readers were resolved in a separate consensus reading; these results were used for statistical analysis. During this reading session, maximum standardized uptake value (SUV_{max}) was recorded for each lesion.

The reference standard for this analysis was created by the expert judgment of a board certified radiologist and neuroradiologist with more than two years of experience in integrated PET/MRI under knowledge of histopathologic results as well as radiologic and clinical follow-up. If no further information existed, the most probable diagnosis was determined by using previous examinations and all available clinical information. Each finding was classified as either benign or malignant. Histopathologic workup was available for one lesion, follow-up was available for 37 lesions (clinical follow-up, $n=16$; PET/CT, $n=11$; ultrasonography and clinical follow-up, $n=5$; PET/MRI, $n=4$; combined ultrasonography and scintigraphy, $n=1$) with a mean follow-up time of 493 ± 252 days. In the remaining 16 lesions, the expert reader decided on the most probable diagnosis using the PET/CT and PET/MRI images, previous examinations, and all available clinical information. In two findings, no definite classification was possible by the expert reader. Therefore, these lesions were considered as indeterminate findings in both modalities.

Statistical analysis

For PET/CT and PET/MRI, the initial rating (most likely benign and most likely malignant) was compared to the reference standard and classified as accurate and inaccurate. As an indeterminate finding does not pose a definite diagnosis and demands further investigation, these findings were classified as inaccurate. The differences between the two imaging procedures were assessed for statistical significance using McNemar’s test. A P value <0.05 indicated statistical significance.

Results

Forty-six ^{18}F -FDG-avid lesions (mean SUV_{max} 5.0 ± 1.9 for PET/CT; 5.9 ± 3.0 for PET/MRI) were discovered by both readers in 26 of all analyzed 81 patients. Incidental unilateral tracer uptake of the vocal cord that was detectable on PET/CT in one patient was not detectable on PET/MRI. Here, no signs

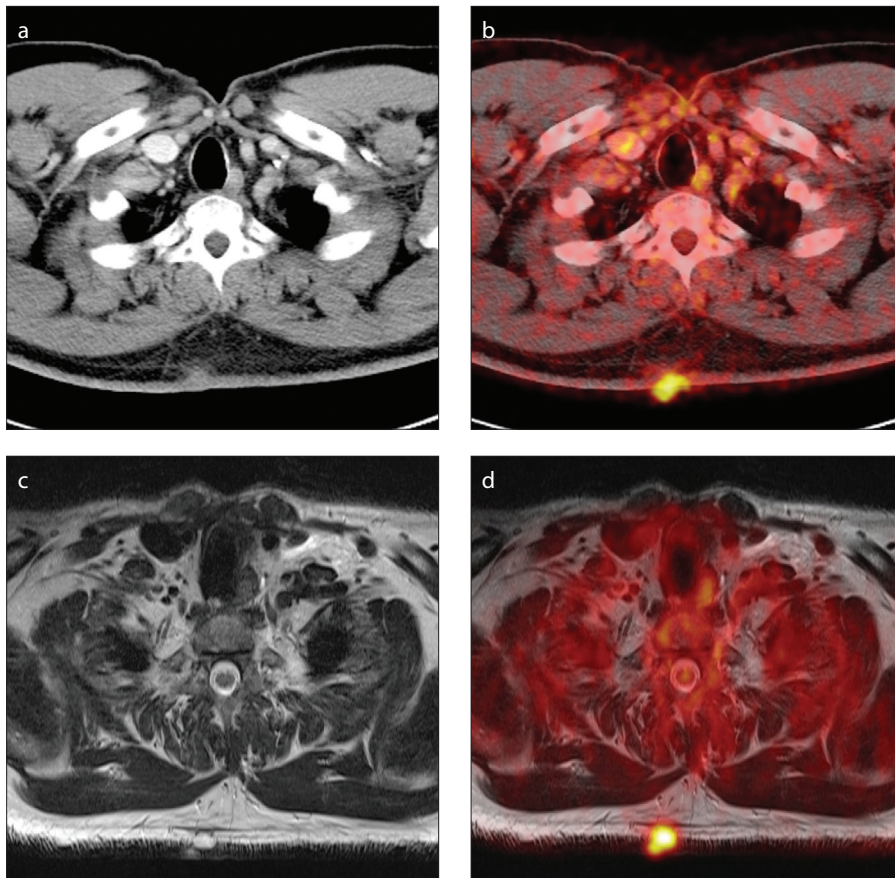


Figure 2. a–d. A 58-year-old male patient who underwent hybrid imaging for staging before ^{131}I -therapy after resection of papillary thyroid cancer. Morphologic and fused images are displayed for PET/CT (a, b) and PET/MRI (c, d). A cutaneous soft-tissue-density lesion in CT image (a) shows a focal tracer uptake (b) and was therefore classified as a cutaneous metastasis. However, on PET/MRI, the high T2-signal indicates an infected sebaceous cyst (c) despite a focal tracer uptake (d). As this lesion showed no change in comparison to prior PET/CT examinations, a metastatic disease was excluded by the expert reader.

of malignancy were detected on follow-up MRI after more than one year.

On PET/CT, 27 lesions were classified as most likely benign, one as most likely malignant, and 18 as indeterminate. On PET/MRI, 31 lesions were classified as most likely benign, one as most likely malignant, and 14 as indeterminate. Forty-three lesions were benign and one lesion was malignant according to the reference standard. In two lesions, a definite diagnosis was not possible due to insufficient follow-up (Table 2). Concerning the correct characterization of incidental ^{18}F -FDG uptake, PET/MRI was not superior to PET/CT ($P = 0.125$). In 28 cases, ^{18}F -FDG uptake was correctly classified by both modalities (Fig. 1). In four cases classified as indeterminate by PET/CT, the underlying inflammatory process could be detected by PET/MRI (Fig. 2).

In 14 lesions, neither PET/CT nor PET/MRI could correctly characterize the increased ^{18}F -FDG uptake. Affected areas were the

larynx and the pharynx ($n=5$), the tonsils ($n=3$), the cervical soft tissue ($n=3$), the axilla ($n=2$), and the thyroid gland ($n=1$). An example of a unilateral tracer uptake in the left vocal cord is displayed in Fig. 3.

Discussion

This study demonstrates a similar performance of PET/CT and PET/MRI when characterizing incidental ^{18}F -FDG uptake in head and neck examinations, despite the superior soft-tissue contrast of PET/MRI.

Due to the complex anatomy in the head and neck area, high-resolution morphologic imaging is crucial for cancer patients. As MRI is superior to CT in terms of accuracy in tumor border delineation and is less susceptible to beam hardening artifacts by dental implants (12–14), many institutions prefer MRI over CT for imaging the head and neck. By combining functional and morphologic imaging, PET/CT is able to increase the sensitivity compared with morphologic imag-

ing alone and has therefore been included in the latest guidelines for head and neck cancer imaging (5, 6). However, local tumor evaluation can be troublesome due to low soft-tissue contrast of CT. Thus, integrated PET/MRI is expected to allow more accurate local tumor staging as well as lymph node evaluation compared with PET/CT. As most data from the literature have to be considered preliminary, no obvious superiority has been demonstrated until today (18–20).

In accordance with the literature on head and neck staging, our data indicate that the superior soft-tissue contrast of PET/MRI does not increase the diagnostic accuracy in the characterization of incidental tracer uptake in the head and neck. This is caused most likely by the high prevalence of functional tracer uptake. Here, the exact anatomical allocation of the PET finding is key to correct classification, which can be realized equally well with contrast-enhanced CT and MRI (21). In addition, most functional tracer uptake is symmetrical and is typically caused by movement and speaking in the uptake phase after tracer injection. This leads to symmetrical pharyngeal and laryngeal enhancement as well as linear uptake of the skeletal musculature, which is considered as physiologic and can be safely ignored without a definite morphologic correlate (22). Furthermore, symmetrical tracer uptake of Waldeyer's ring, the salivary glands, and the thyroid without morphologic correlate is frequently observed and does not indicate an underlying pathology (23, 24). Another frequent cause for symmetrical tracer uptake is brown fatty tissue (22, 25). Due to excellent spatial registration of the CT and MRI images and the PET dataset, symmetrical tracer uptake could be attributed precisely to the corresponding tissue in this study by PET/CT and PET/MRI.

Asymmetrical or unilateral ^{18}F -FDG uptake in the head and neck area is of special interest as it might indicate a malignant tumor. Although increased, unilateral glucose metabolism can be caused by inflammatory processes or asymmetrical focal muscular activity and has to be considered as nonspecific in most cases, it can mimic malignant processes (26, 27). Heusner et al. (27) demonstrated that unilateral or asymmetrical muscular uptake without a morphologic correlate is no predictor for malignancy. Still, its presence can be problematic in some cases, particularly if the quality of morphologic images is impaired by motion

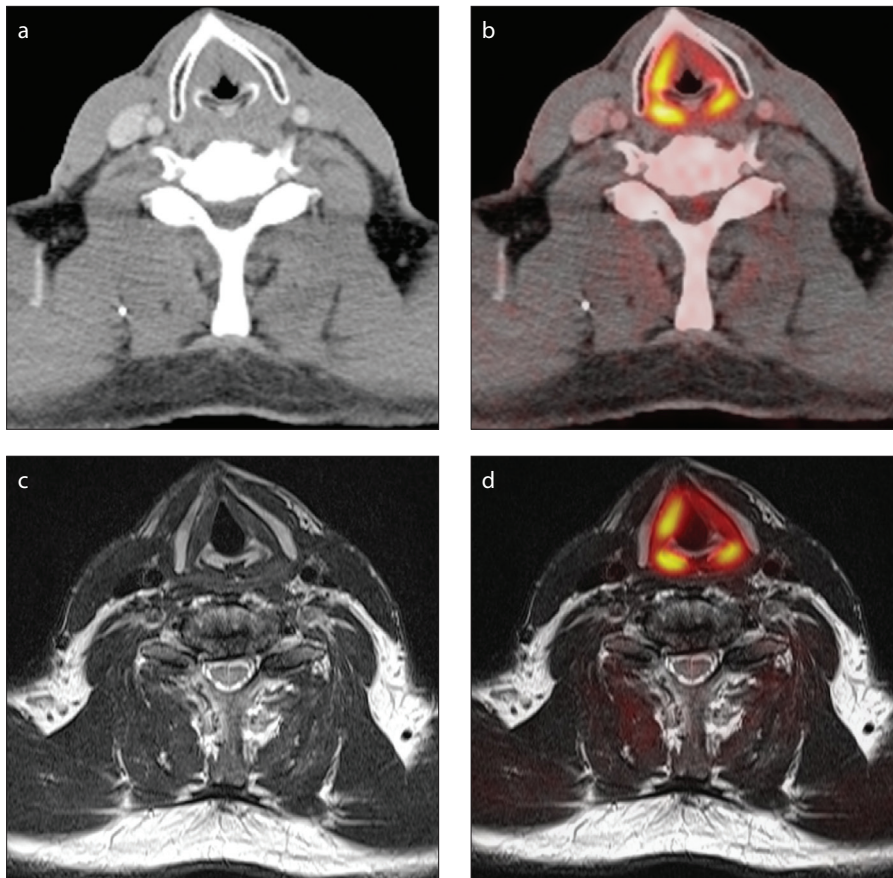


Figure 3. a–d. A 56-year-old male patient who underwent hybrid imaging for initial staging of oropharyngeal cancer. Morphologic and fused images are displayed for PET/CT (a, b) and PET/MRI (c, d). Although no lesion can be found in CT (a) and MRI (c) exams, a strong focal tracer uptake in the right vocal cord is visible (b, d). During follow-up, no malignancy was observed at this site.

artifacts and a morphologic correlate cannot be safely excluded.

In the thyroid, focal tracer uptake is problematic. Although Choi et al. (28) found increased focal tracer uptake to be a strong predictor for malignancy, more recent studies showed that also benign nodules show a strong tracer uptake and that the frequency of malignant nodules is lower than initially reported (29). Still, focal asymmetrical ^{18}F -FDG uptake in the thyroid demands further investigation (25, 29, 30). Unfortunately, MRI is not superior to CT in the differentiation between benign and malignant thyroid lesions (31). This can also be observed in our study: while one large thyroid nodule could be classified correctly as malignant by PET/CT and PET/MRI due to an inhomogeneous appearance and a blurred delineation, both methods failed to provide a definite diagnosis in a small thyroid lesion that showed no signs of malignancy in more than one year of clinical follow-up.

Hence, the considerable percentage of indeterminate incidental tracer uptake in

this study demonstrates that hybrid imaging always has to be considered only as a part of the diagnostic process in head and neck malignancies. A careful clinical examination prior to a hybrid imaging examination is therefore of utmost importance and can further improve the accuracy of both PET/CT and PET/MRI. Furthermore, correlation of hybrid imaging examinations with other imaging modalities such as ultrasonography or scintigraphy might be helpful.

This study has some minor limitations. Apart from its retrospective character, the cohort is relatively small and includes various tumor entities. Therefore, these results have to be considered as preliminary and further investigations in larger cohorts are required. Although histopathologic verification for each lesion cannot be obtained due to various clinical and ethical reasons, the inclusion of an expert reader who performed the classification under knowledge of all clinical information including histopathologic sampling and follow-up examinations has to be considered as a limitation of this study.

Different imaging time points after tracer injection for PET/CT and PET/MRI can lead to differences in tracer accumulation and influence sensitivity. However, this was only observed in one lesion and we believe that in future, either PET/CT or PET/MRI will be performed and that both modalities will not be performed subsequently. Furthermore, there is a discrepancy of reading experience between PET/MRI and PET/CT in all readers which cannot be avoided due to the later commercial availability of PET/MRI.

In conclusion, the present data indicate that ^{18}F -FDG PET/MRI is not able to reduce the number of indeterminate findings in the head and neck examinations compared with PET/CT.

Conflict of interest disclosure

The authors declared no conflicts of interest.

References

- Antoch G, Vogt FM, Freudenberg LS, et al. Whole-body dual-modality PET/CT and whole-body MRI for tumor staging in oncology. *JAMA* 2003; 290:3199–3206. [\[CrossRef\]](#)
- Antoch G, Saudi N, Kuehl H, et al. Accuracy of whole-body dual-modality fluorine-18-2-fluoro-2-deoxy-d-glucose positron emission tomography and computed tomography (FDG-PET/CT) for tumor staging in solid tumors: comparison with CT and PET. *J Clin Oncol* 2004; 22:4357–4368. [\[CrossRef\]](#)
- Antoch G, Statta J, Nemat AT, et al. Non-small cell lung cancer: dual-modality PET/CT in preoperative staging. *Radiology* 2003; 229:526–533. [\[CrossRef\]](#)
- Rosenbaum SJ, Lind T, Antoch G, et al. False-positive FDG PET uptake—the role of PET/CT. *Eur Radiol* 2006; 16:1054–1065. [\[CrossRef\]](#)
- Wolff K-D, Follmann M, Nast A. The diagnosis and treatment of oral cavity cancer. *Dtsch Arztebl Int* 2012; 109:829–835.
- Grégoire V, Lefebvre J-L, Licitra L, Felip E. Squamous cell carcinoma of the head and neck: EHNS-ESMO-ESTRO Clinical Practice Guidelines for diagnosis, treatment and follow-up. *Ann Oncol* 2010; 21:184–186. [\[CrossRef\]](#)
- Schaaf WEJ, Patel Z, Retrouvey M, et al. Frequency and clinical relevance of PET/CT incidentalomas. *Abdom Imaging* 2014; 39:657–662. [\[CrossRef\]](#)
- Wong W-L, Gibson D, Sanghera B, et al. Evaluation of normal FDG uptake in palatine tonsil and its potential value for detecting occult head and neck cancers: A PET CT study. *Nucl Med Commun* 2007; 28:675–680. [\[CrossRef\]](#)
- Sebro R, Aparici C, Pampaloni M. Frequency and clinical implications of incidental new primary cancers detected on true whole-body ^{18}F -FDG PET/CT studies. *Nucl Med Commun* 2013; 34:333–339. [\[CrossRef\]](#)
- Al-Hakami HA, Makis W, Anand S, et al. Head and neck incidentalomas on positron emission tomographic scanning: ignore or investigate? *J Otolaryngol* 2011; 40:384–390.

11. Patel A, Perry T, Hunt I, et al. Should we routinely investigate incidental head and neck findings on 18-fluorodeoxyglucose positron emission tomography in patients being staged for non-small cell lung cancer? A retrospective analysis. *Thorac Cardiovasc Surg* 2015; 63:604–608.
12. Held P, Breit A. MRI and CT of tumors of the pharynx: comparison of the two imaging procedures including fast and ultrafast MR sequences. *Eur J Radiol* 1994; 18:81–91. [\[CrossRef\]](#)
13. Sigal R, Zagdanski AM, Schwaab G, et al. CT and MR imaging of squamous cell carcinoma of the tongue and floor of the mouth. *Radiographics* 1996; 16:787–810. [\[CrossRef\]](#)
14. Leslie A, Fyfe E, Guest P, et al. Staging of squamous cell carcinoma of the oral cavity and oropharynx: a comparison of MRI and CT in T- and N-staging. *J Comput Assist Tomogr* 1999; 23:43–49. [\[CrossRef\]](#)
15. Buchbender C, Heusner TA, Lauenstein TC, et al. Oncologic PET/MRI, Part 1: Tumors of the brain, head and neck, chest, abdomen, and pelvis. *J Nucl Med* 2012; 53:928–938. [\[CrossRef\]](#)
16. Loeffelbein DJ, Souvatzoglou M, Wankerl V, et al. PET-MRI fusion in head-and-neck oncology: current status and implications for hybrid PET/MRI. *J Oral Maxillofac Surg* 2012; 70:473–483. [\[CrossRef\]](#)
17. Schaarschmidt BM, Grueneisen J, Heusch P, et al. Does 18F-FDG PET/MRI reduce the number of indeterminate abdominal incidentalomas compared with 18F-FDG PET/CT? *Nucl Med Commun* 2015; 36:588–595. [\[CrossRef\]](#)
18. Kubiessa K, Purz S, Gawlitza M, et al. Initial clinical results of simultaneous 18F-FDG PET/MRI in comparison to 18F-FDG PET/CT in patients with head and neck cancer. *Eur J Nucl Med Mol Imaging* 2014; 41:639–648. [\[CrossRef\]](#)
19. Partovi S, Kohan A, Vercher-Conejero JL, et al. Qualitative and quantitative performance of 18F-FDG-PET/MRI versus 18F-FDG-PET/CT in patients with head and neck cancer. *Am J Neuroradiol* 2014; 35:1970–1975. [\[CrossRef\]](#)
20. Schaarschmidt BM, Heusch P, Buchbender C, et al. Locoregional tumour evaluation of squamous cell carcinoma in the head and neck area: a comparison between MRI, PET/CT and integrated PET/MRI. *Eur J Nucl Med Mol Imaging* 2016; 43:92–102. [\[CrossRef\]](#)
21. Kostakoglu L, Hardoff R, Mirtcheva R, et al. PET-CT fusion imaging in differentiating physiologic from pathologic FDG uptake. *Radiographics* 2004; 24:1411–1431. [\[CrossRef\]](#)
22. Blodgett TM, Fukui MB, Snyderman CH, et al. Combined PET-CT in the head and neck. *Radiographics* 2005; 25:897–912. [\[CrossRef\]](#)
23. Shreve PD, Anzai Y, Wahl RL. Pitfalls in oncologic diagnosis with FDG PET imaging: physiologic and benign variants. *Radiographics* 1999; 19:61–77. [\[CrossRef\]](#)
24. Goerres GW, Kamel E, Seifert B, et al. Accuracy of image coregistration of pulmonary lesions in patients with non-small cell lung cancer using an integrated PET/CT system. *J Nucl Med* 2002; 43:1469–1475.
25. Purohit BS, Ailianou A, Dulguerov N, et al. FDG-PET/CT pitfalls in oncological head and neck imaging. *Insights Imaging* 2014; 5:585–602. [\[CrossRef\]](#)
26. Goerres GW, von Schulthess GK, Hany TF. Positron emission tomography and PET CT of the head and neck: FDG uptake in normal anatomy, in benign lesions, and in changes resulting from treatment. *AJR Am J Roentgenol* 2002; 179:1337–1343. [\[CrossRef\]](#)
27. Heusner TA, Hahn S, Hamami ME, et al. Incidental head and neck 18F-FDG uptake on PET/CT without corresponding morphological lesion: early predictor of cancer development? *Eur J Nucl Med Mol Imaging* 2009; 36:1397–1406. [\[CrossRef\]](#)
28. Choi JY, Lee KS, Kim H-J, et al. Focal thyroid lesions incidentally identified by integrated 18F-FDG PET/CT: clinical significance and improved characterization. *J Nucl Med* 2006; 47:609–615.
29. King DL, Stack BC, Spring PM, et al. Incidence of thyroid carcinoma in fluorodeoxyglucose positron emission tomography-positive thyroid incidentalomas. *Otolaryngol Head Neck Surg* 2007; 137:400–404. [\[CrossRef\]](#)
30. Boeckmann J, Bartel T, Siegel E, et al. Can the pathology of a thyroid nodule be determined by positron emission tomography uptake? *Otolaryngol Head Neck Surg* 2012; 146:906–912. [\[CrossRef\]](#)
31. Hoang JK, Langer JE, Middleton WD, et al. Managing incidental thyroid nodules detected on imaging: white paper of the ACR incidental thyroid findings committee. *J Am Coll Radiol* 2015; 12:143–150. [\[CrossRef\]](#)